



Generalized Volume-Complexity for a RN-AdS Black Hole



Meng-Ting Wang

Institute of Theoretical Physics, Lanzhou University



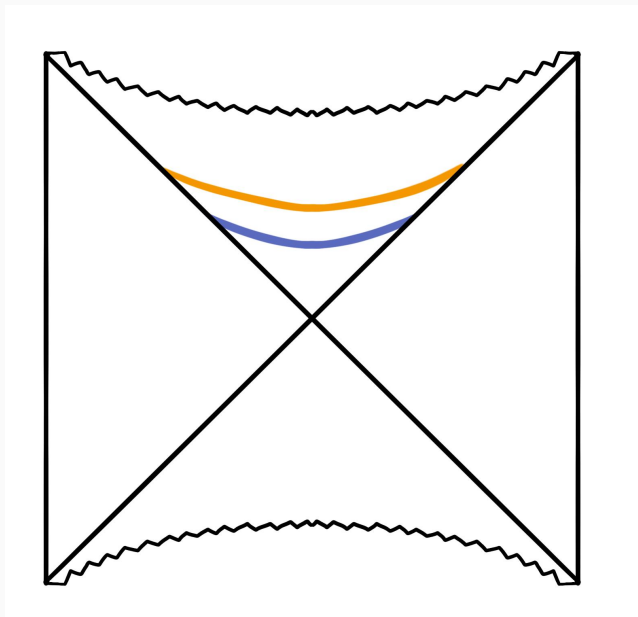
Based on: M.-T.Wang, H.-Y.Jiang, and Y.-X.Liu,
arXiv:2304.05751 [hep-th].



APSW-GC, May 17th

Introduction

The AdS/CFT correspondence provides the ground for kinds of conjectures about the connections between quantum information and quantum gravity.



Entanglement is not enough

What is dual to the wormhole length?

L. Susskind, Fortsch. Phys. 64 (2016) 49

Figure 1. The Penrose diagram of the AdS spacetime.

Introduction

Holographic complexity was proposed to describe the late volume growth of the Einstein-Rosen bridge, and a series of proposals were put forward.

complexity = volume
(CV)

$$C_V \sim \frac{V}{G_N l_{bulk}}$$

D. Stanford and L. Susskind, Phys. Rev. D 90 (2014) 126007

complexity = action
(CA)

$$C_A \sim \frac{A_{WdW}}{\pi \hbar}$$

A. R. Brown, D. A. Roberts, Phys. Rev. Lett. 116 (2016) 191301

complexity = spacetime
volume (CV2.0)

$$C_{SV} \sim \frac{V}{G_N l_{bulk}^2}$$

J. Couch, W. Fischler, and P. H. Nguyen, JHEP 03 (2017) 119

Introduction

Complexity = Volume (CV): the complexity is dual to the volume of the extremal (maximal) hypersurface anchored at boundary times $t_R = t_L = \tau/2$ (consider symmetry)

$$C_V \sim \frac{V}{G_N l_{bulk}},$$

where G_N denotes Newton's constant in the bulk gravitational theory. For simplicity, choose $l_{bulk} = L$, i.e., the curvature radius of AdS.

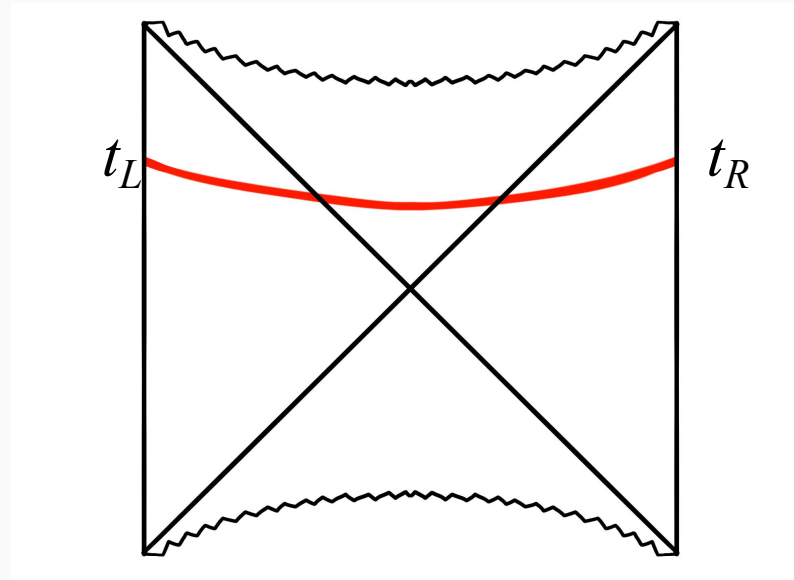


Figure 2. The Penrose diagram of the AdS spacetime.

Introduction

In general, one can summarize the CV proposal in two steps. Recently, a broad new class of gravitational observables have been proposed to provide new possibilities for holographic complexity in the same way.

A. Belin, R. C. Myers, S. M. Ruan, G. Sárosi, and A. J. Speranza, Phys. Rev. Lett. 128 (2022)

First. The maximization procedure

$$\delta_x \left[\int_{\Sigma} d^d \sigma \sqrt{h} F_2(g_{\mu\nu}; X^\mu) \right] = 0$$

Second. Evaluating a particular geometric feature of this special hypersurface

$$O_{F_1, \Sigma_{F_2}}(\Sigma_{CFT}) = \frac{1}{G_N L} \int_{\Sigma_{F_2}} d^d \sigma \sqrt{h} F_1(g_{\mu\nu}; X^\mu)$$

The new scalar functionals F_1 and F_2 depend on the bulk metric and the embedding functions.

The generalized volume for the 4D charged AdS black hole

The infalling Eddington-Finkelstein coordinates for the 4D RN-AdS black hole:

$$ds^2 = -f(r)dv^2 + 2dvdr + r^2d\Omega^2$$

$$f(r) = 1 - \frac{2M}{r} + \frac{Q^2}{r^2} + \frac{r^2}{L^2}$$

$$v = t + r_*(r)$$

$$r_*(r) = - \int_r^\infty f(r')^{-1} dr'$$

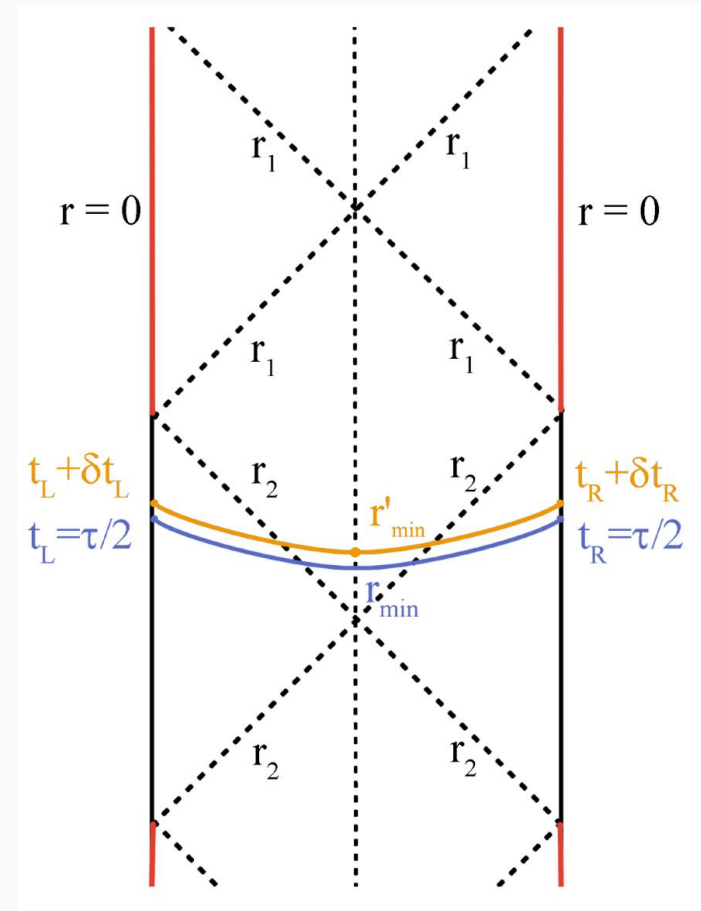


Figure 3. The Penrose diagram of the RN-AdS spacetime. When t_L is shifted to $t_L + \delta t_L$, the extreme hypersurface evolves from the blue curve to the yellow curve.

The generalized volume for the 4D charged AdS black hole

Choosing the scalar functionals

$$F_1 = F_2 = a(r) = 1 + \lambda L^4 C^2$$

$C^2 \equiv C_{\mu\nu\rho\sigma} C^{\mu\nu\rho\sigma}$ the square of the Weyl tensor λ dimensionless parameter

The observable can be seen as a generalization of the volume-complexity duality and, therefore, is referred to as the **generalized volume** C_{gen} :

$$C_{gen} = \frac{V_0}{G_{NL}} \int_{\Sigma_{F_2}} d\sigma r^2 \sqrt{-f(r)\dot{v}^2 + 2\dot{v}\dot{r}} a(r).$$

Since C_{gen} is translationally invariant in the coordinate v , we can obtain the conserved quantity

$$\frac{\partial L}{\partial \dot{v}} = r^2 \frac{(\dot{r} - f(r)\dot{v})a(r)}{\sqrt{-f(r)\dot{v}^2 + 2\dot{v}\dot{r}}} \equiv P_v.$$

Maximization procedure to the effective potential theory

$$\frac{\partial L}{\partial \dot{v}} = r^2 \frac{(\dot{r} - f(r)\dot{v})a(r)}{\sqrt{-f(r)\dot{v}^2 + 2\dot{v}\dot{r}}} \equiv P_v$$

$$\sqrt{-f(r)\dot{v}^2 + 2\dot{v}\dot{r}} = a(r)r^2$$

$$P_v = \dot{r} - f(r)\dot{v}$$

$$\dot{r} = \pm \sqrt{P_v^2 + f(r)a^2(r)r^4}$$

$$\dot{r}^2 + U(r) = P_v^2$$

Effective potential

$$U(r) = -f(r)a^2(r)r^4$$

The generalized volume for the 4D charged AdS black hole

Relation between the boundary time τ and conserved momentum P_v

$$\tau = 2t_R = -2 \int_{r_\epsilon}^{r_{min}} \frac{P_v}{f(r)\sqrt{P_v^2 - U(r)}} dr$$

Linear growth rate at late times

$$\lim_{\tau \rightarrow \infty} \frac{dC_{gen}}{d\tau} \sim \lim_{\tau \rightarrow \infty} P_v(\tau) \equiv P_{crt}$$

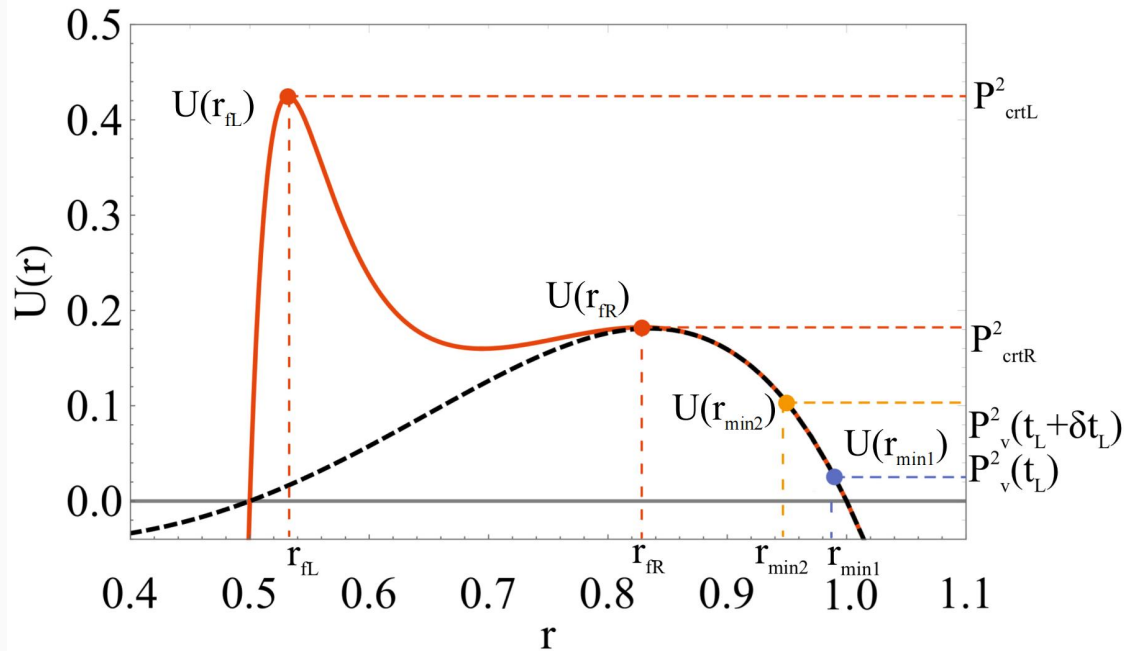
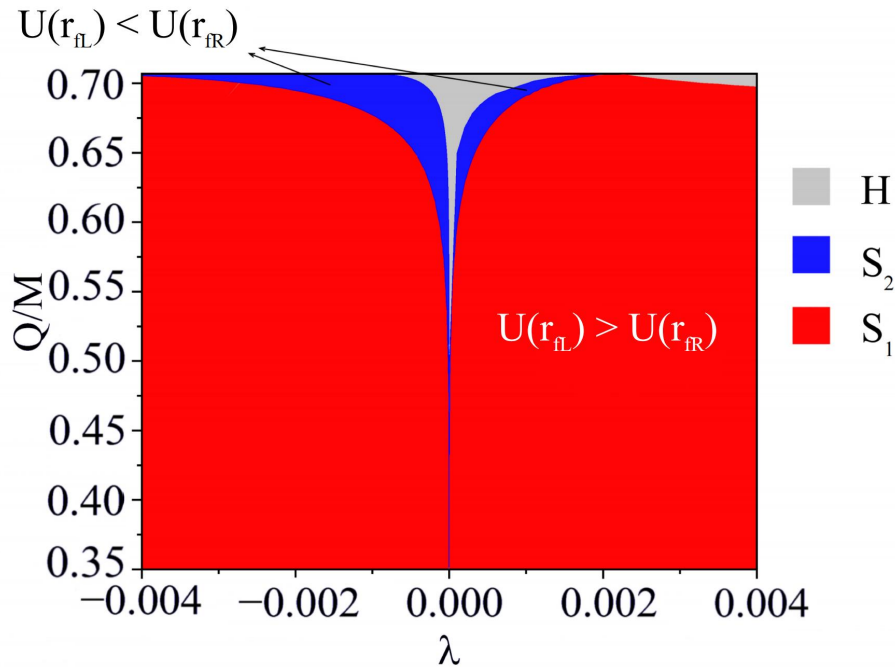
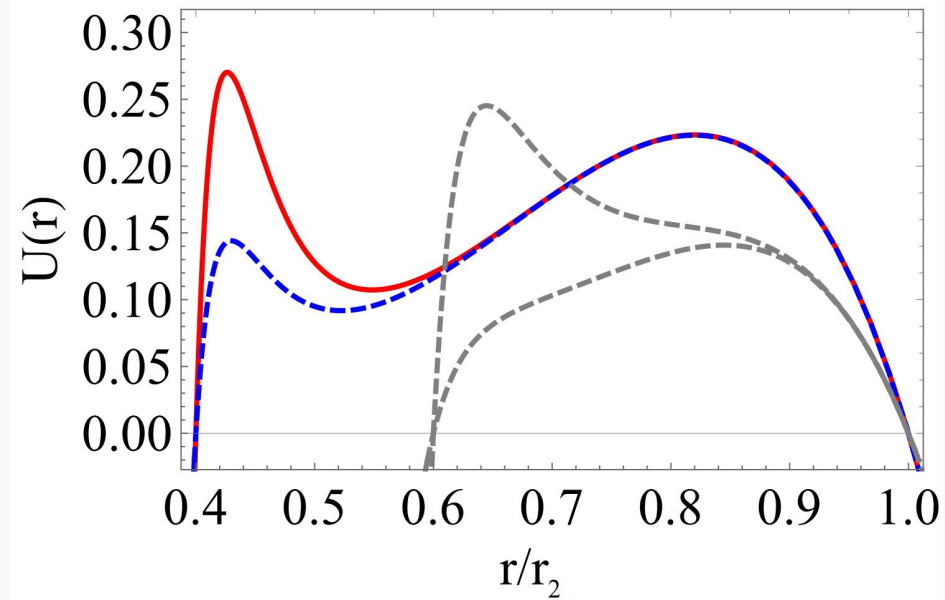


Figure 4. The effective potential U as a function of the radial coordinate with $r_1/r_2 = 0.5$, $L/r_2 = 1$, and $\lambda = 0.002$ and 0.0 . When $\lambda = 0$, the generalized volume degenerates to the volume V . The black dashed curve represents the potential obtained from the volume.

Effective potential with two local maximum and turning time



5(a)



5(b)

Figure 5. Left: The parameter space of the number of the local maxima of the effective potential $U(r)$ between the two horizons of the black hole with $L/r_2 = 1$. Right: The effective potential $U(r)$ with $L/r_2 = 1$. The red curve corresponds to $r_1/r_2 = 0.4$ and $\lambda = 0.0006$. The blue dashed curve corresponds to $r_1/r_2 = 0.4$ and $\lambda = 0.0004$. The grey dashed curves correspond to $r_1/r_2 = 0.6$ and $\lambda = 0.001, 0.003$.

Effective potential with two local maximum and turning time

For an infinite boundary time $\tau \rightarrow \infty$, we obtain more than one different extremal hypersurfaces. These different extremal hypersurfaces have different late-time linear growth rates P_{crtL} and P_{crtR} .

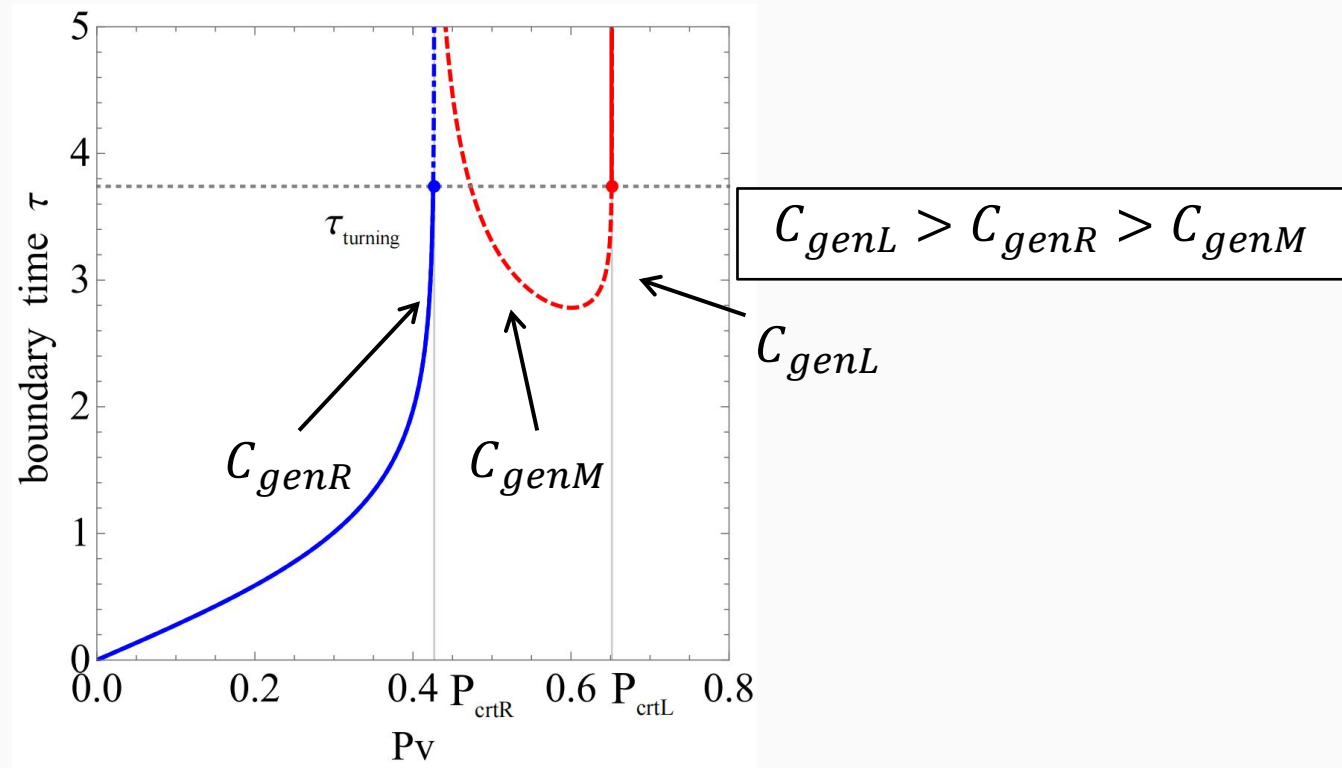


Figure 6. The relation between the boundary time τ and the conserved momentum P_v with $r_1/r_2 = 0.5$, $L/r_2 = 1$, $\lambda = 0.002$.

Effective potential with two local maximum and turning time

When the hypersurface evolves with the boundary time τ , there will be a turning time τ_{turning} . Before the turning time, the generalized volume C_{genL} is smaller than C_{genR} , but after the turning time, the generalized volume C_{genL} is larger than C_{genR} .

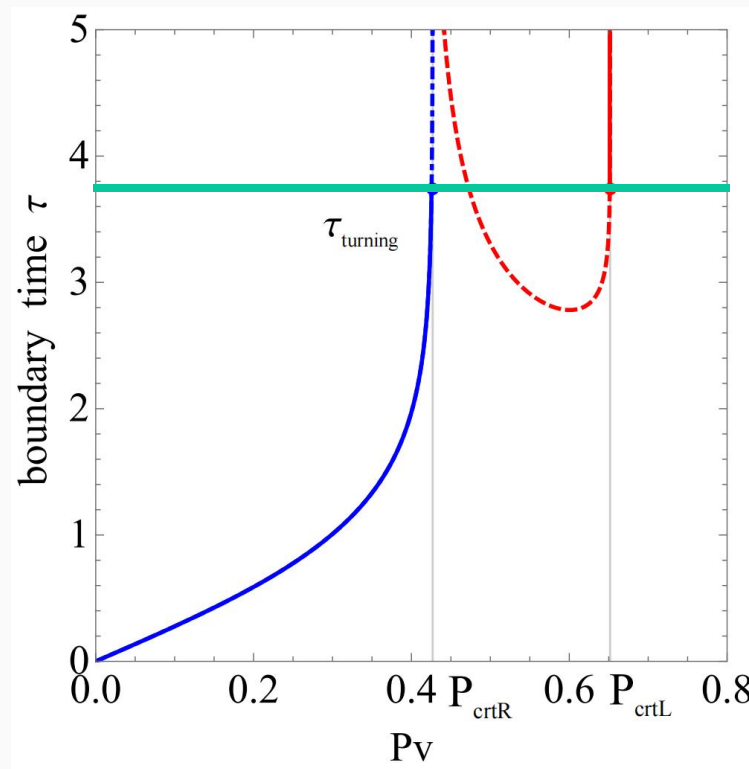


Figure 6. The relation between the boundary time τ and the conserved momentum P_v with $r_1/r_2 = 0.5$, $L/r_2 = 1$, $\lambda = 0.002$.

Effective potential with two local maximum and turning time

For the extremal hypersurface that has the minimum radius between the two horizons of the black hole, if the time to reach the boundary is always positive, as shown in left. Three hypersurfaces for one boundary time τ .

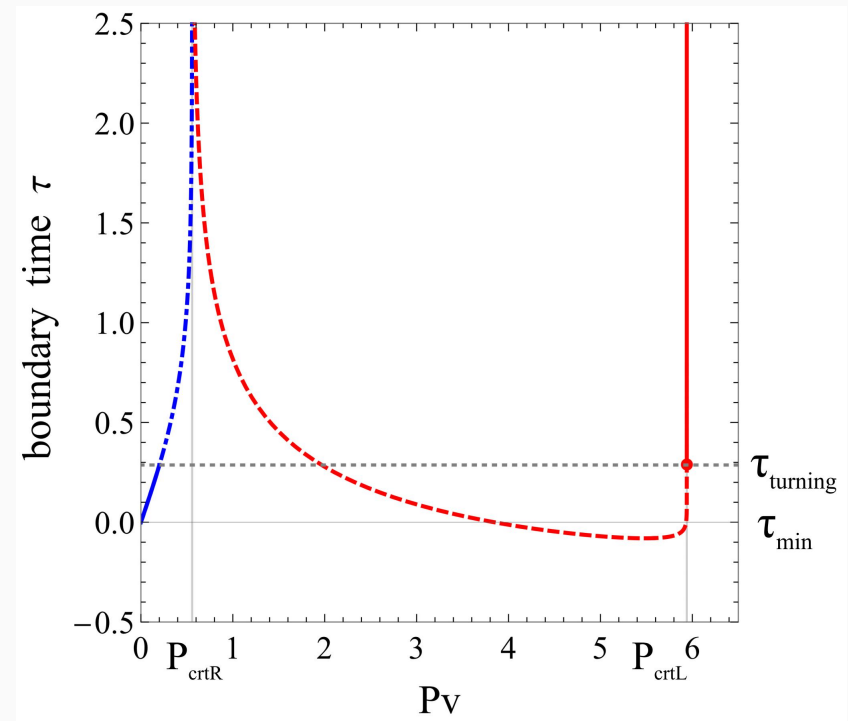
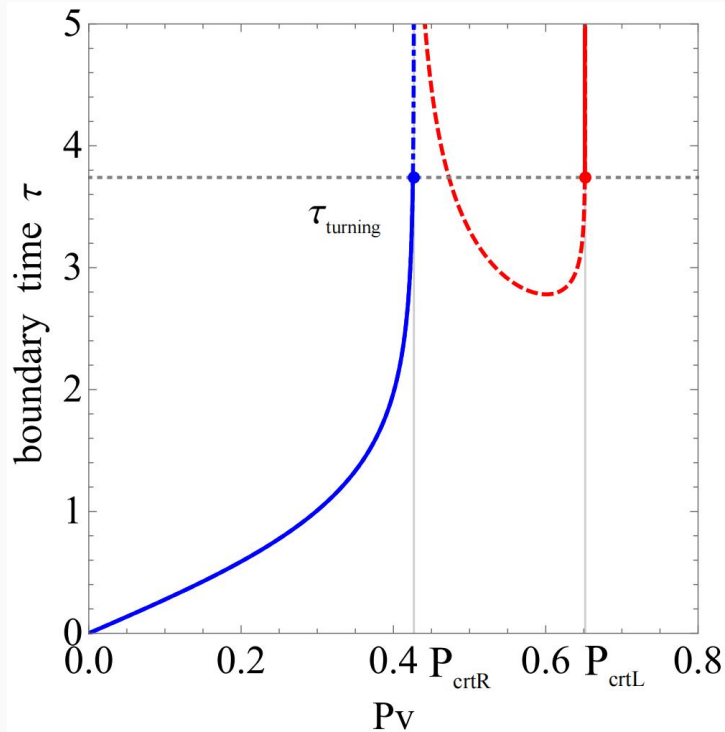


Figure 7. The relation between the boundary time τ and the conserved momentum P_v .

Left: $r_1/r_2 = 0.5$, $L/r_2 = 1$, $\lambda = 0.002$. Right: $r_1/r_2 = 0.18$, $L/r_2 = 1$, and $\lambda = 0.00025$.

Effective potential with two local maximum and turning time

When $\tau > |\tau_{\min}|$, we can obtain three extreme surfaces for the same boundary time, as shown in left.

Because of the reflection symmetry. When $\tau < |\tau_{\min}|$, we can obtain five extreme surfaces for the same boundary time, as shown in right, where the dotted line represents the time reflected trajectory.

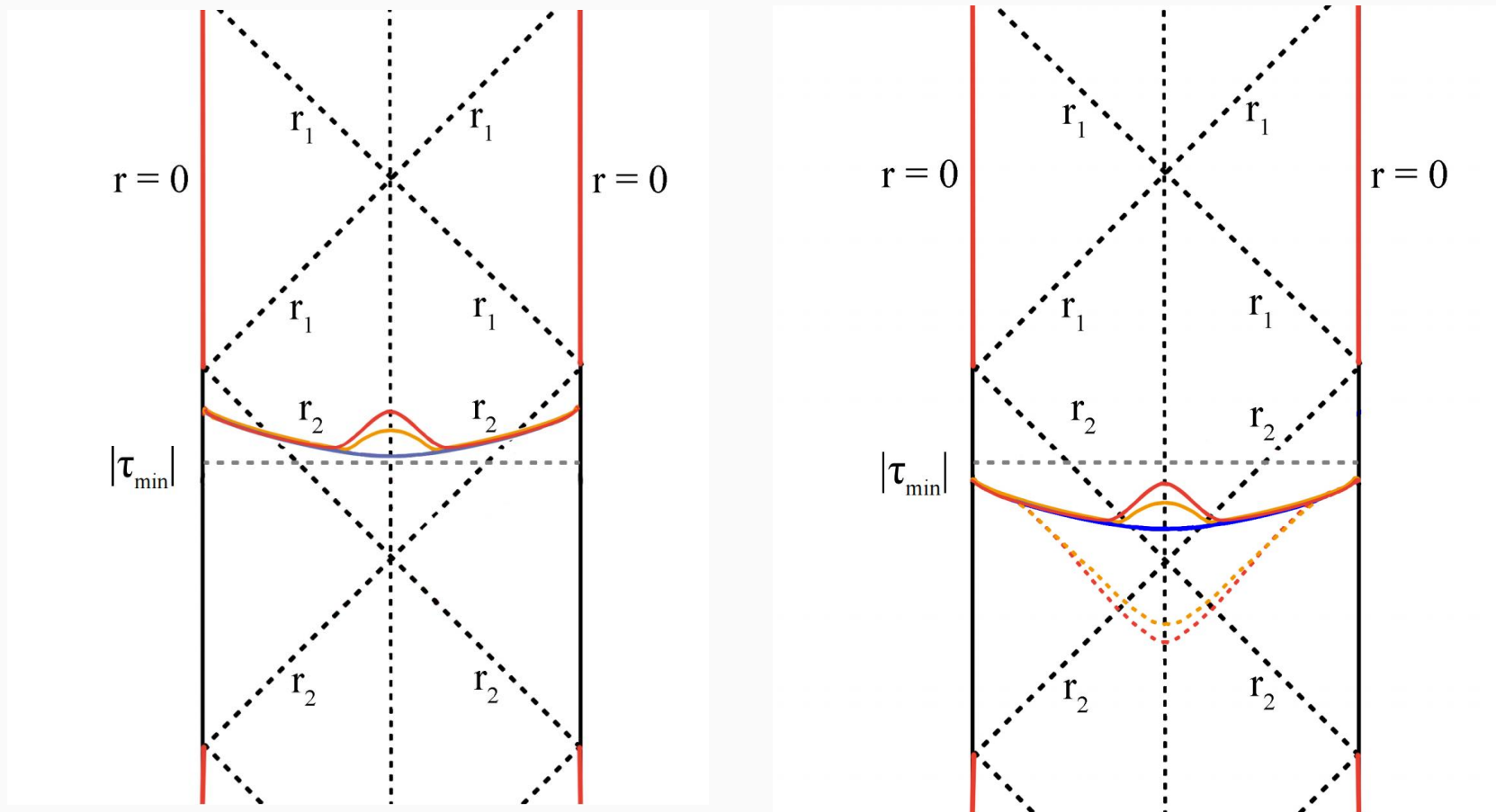


Figure 9. Penrose diagram for the RN-AdS spacetime, Left: $\tau > |\tau_{\min}|$; Right: $\tau < |\tau_{\min}|$.

Effective potential with two local maximum and turning time

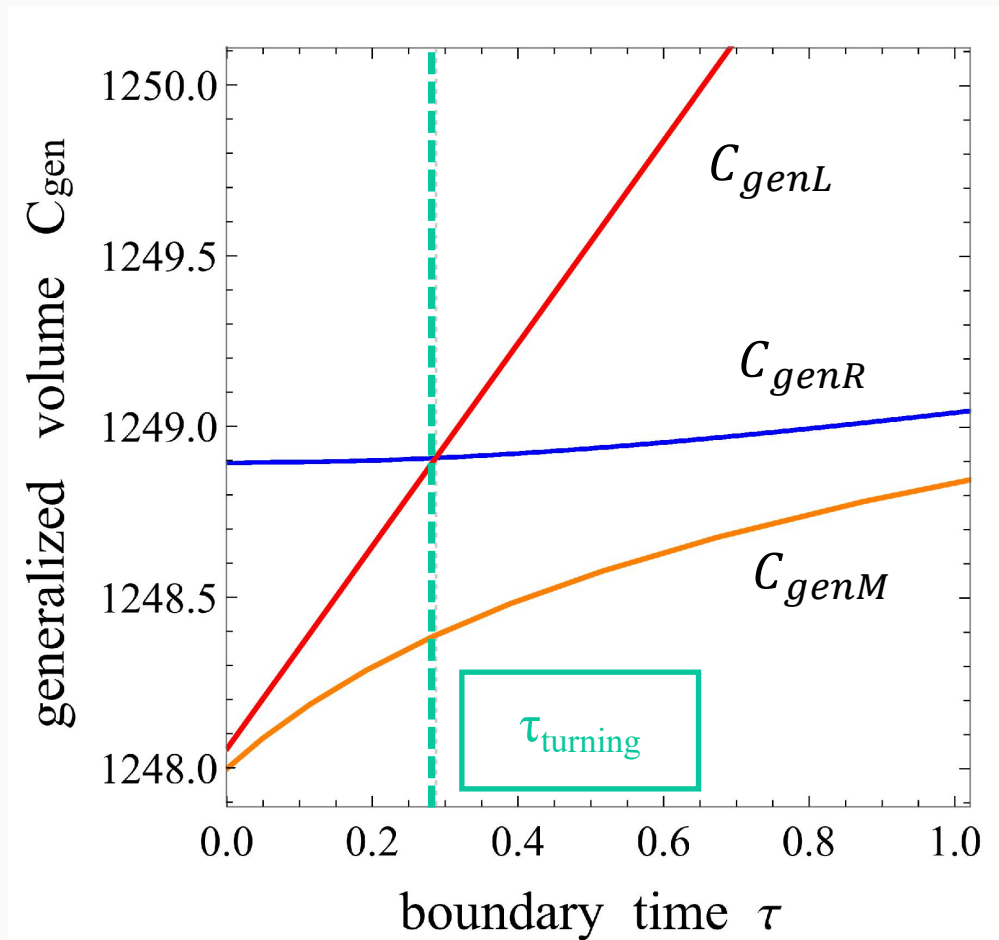


Figure 10. The relation between the generalized volume C_{gen} and the boundary time τ with $L/r_2 = 1$, $r_1/r_2 = 0.18$, $r_\epsilon/r_2 = 500$ and $\lambda = 0.00025$.

Conclusion

- We investigate generalized volume-complexity for the 4-dimensional Reissner-Nordström-AdS black hole.
- These new observables satisfy the characteristic of the thermofield double state, i.e., they grow linearly in time on the late stage.
- We find that there are multiple extremal hypersurfaces anchored at a certain boundary time.
- New definition: we call the time when one hypersurface replaces another to become the largest extreme hypersurface the turning time τ_{turning} .





Thank you for listening!